International Journal of Electrical, Electronic and Communication Sciences
ISSN: 2517-9438
Vol:11, No:8, 2017

A Model Predictive Control Based Virtual Active Power Filter Using V2G Technology

Mahdi Zolfaghari, Seyed Hossein Hosseinian, Hossein Askarian Abyaneh, Mehrdad Abedi

***Abstract*—**This paper presents a virtual active power filter (VAPF) using vehicle to grid (V2G) technology to maintain power quality requirements. The optimal discrete operation of the power converter of electric vehicle (EV) is based on recognizing desired switching states using the model predictive control (MPC) algorithm. A fast dynamic response, lower total harmonic distortion (THD) and good reference tracking performance are realized through the presented control strategy. The simulation results using MATLAB/Simulink validate the effectiveness of the scheme in improving power quality as well as good dynamic response in power transferring capability.

***Keywords*—**Virtual active power filter, V2G technology, model predictive control, electric vehicle, power quality.

I. Introduction

THE widespread use of electronic equipment, such as information technology equipment, power electronics based optimal speed/torque controller of electrical motor, smart lighting, has changed the behaviour of electric loads. The nonlinear nature of these deformed loads has caused many power quality problems. Due to their non-linearity, all of these loads cause disturbances in the voltage waveform. To remove the effects of these loads and acceptable power quality, several structures of power filters i.e., passive [1], shunt [2]-[4], series, and combination of shunt and series active filters with passive components [5]-[7] have been presented as solutions in a polluted electric network. Among active filter topologies, SAPF (shunt active power filter) with its naive implementation is paid more attention in both time and frequency domains to facilitate the compensation of harmonic currents and reactive power of non-linear loads [8], [9]. In [10], a digital implementation of fuzzy control algorithm has been presented for the SAPF in power system. A method is presented in [11] for the control of a three-level neutral-point clamped converter and the injection of harmonic current components of nonlinear loads. The method can also guarantee a unity power factor for the utility grid. A control plan also was presented in [12] to reject the uncertainties from the power grid. Several studies [13]-[18] indicated that EVs may profitably provide power to the grid when they are parked and connected to an electrical outlet. This process is called V2G technology. There are three types of EVs – battery, fuel cell, and plug-in hybrid– and they have been used to provide power for base load, peak power, and also they act as storage systems for renewable energy sources with intermittent behaviour [19]. The purpose of V2G technology is that EV delivers electric power to the utility when the PV is parked. In order to deliver electric power to the grid, each EV must have three required elements as follows: (a) a power connection to the grid for electrical energy flow, (b) control or logical connection necessary for communication with grid operators, and (c) precision metering on-board the vehicle. So far, the use of V2G and G2V (Grid-to-vehicle) technologies in power system applications has been reported in various studies. For instance, [20] has considered the EVs as virtual static compensator (STATCOM) for reactive power compensation purposes. A virtual unified power flow controller (UPFC) using V2G technology has also been reported in [21]. The authors of [22] have also used the EVs to reduce the losses and to smoothing of the load duration curves in distribution system. To solve the power quality issues of a wind power unit, [23] has benefited from implementing the EVs in the output bus of the wind power unit, near to the sensitive loads. The study presented in [24], based on the p-q theory, considered the EVs to reduce the power quality problems caused by a HVDC system.

In this paper, we utilize the EV as a VAPF to improve the power quality. In the proposed method, the converter of EV is controlled using a MPC algorithm. The rest of the paper is organized as follows: Section II describes the system structure and dynamic model of the EV battery. The proposed control strategy of EV as a virtual active filter is given in Section III. The simulation results are provided in Section IV to verify the performance of the proposed strategy. Finally, the conclusion is presented in Section V.

II. System Structure and Dynamic Modeling

Overall power circuit of the system is drawn in Fig. 1. The EV battery, as shown, is connected to the power grid through a power converter that operates in inverter mode based on V2G concept. The subsequent sections describe the dynamic modeling of the EV battery and the working principle of the inverter.

A. EV Battery Model

In this study, since EVs are able to compensate reactive power to utility grid as introduced in [20], they are considered as dynamic batteries which are connected to the system through bidirectional converters [25]. For each EV, a dynamic model of

M. Zolfaghari, Ph.D. student in Electrical Engineering, S. H. Hosseinian, H. Askarian Abyaneh, and M. Abedi are with the Department of Electrical Engineering, Tehran Polytechnic, Tehran, Iran (e-mail: mahdizolfaghari@aut.ac.ir, Hosseinian@aut.ac.ir, Askarian@aut.ac.ir, abedi@aut.ac.ir).

a rechargeable battery is used. This model was described in [26], in which a dynamic lithium-ion battery model considering the effects of temperature and capacity fading was presented. Here, this model is adopted because of its good and exact dynamic response during charge and recharge process. The output voltage of the battery is obtained as [26];

$$V_{bat} = V_{OC} - i_{bat} Z_{eq} + \Delta E(T) \quad (1)$$

where, V_{OC} is the battery open circuit voltage, i_{bat} battery current, Z_{eq} the internal impedance of battery, and $\Delta E(T)$ is temperature correction of the potential. The equivalent impedance Z_{eq} is shown in Fig. 2. In this figure, R_{series} is responsible for the instantaneous voltage drops in battery terminal voltage. The other component of series resistor R_{cycle}, indicates that the internal impedance of the battery is increased with each cycle of discharging operation. All of these components are a function of state of charge (SOC). Also, the value of battery open circuit voltage V_{OC} is strongly dependent on battery SOC that can be calculated as;

$$SOC = SOC_{\text{int}} - \int (i_{Battery} / C_{usable}) dt \quad (2)$$

where SOC_{int} is the initial value of SOC. More details are presented in [26].

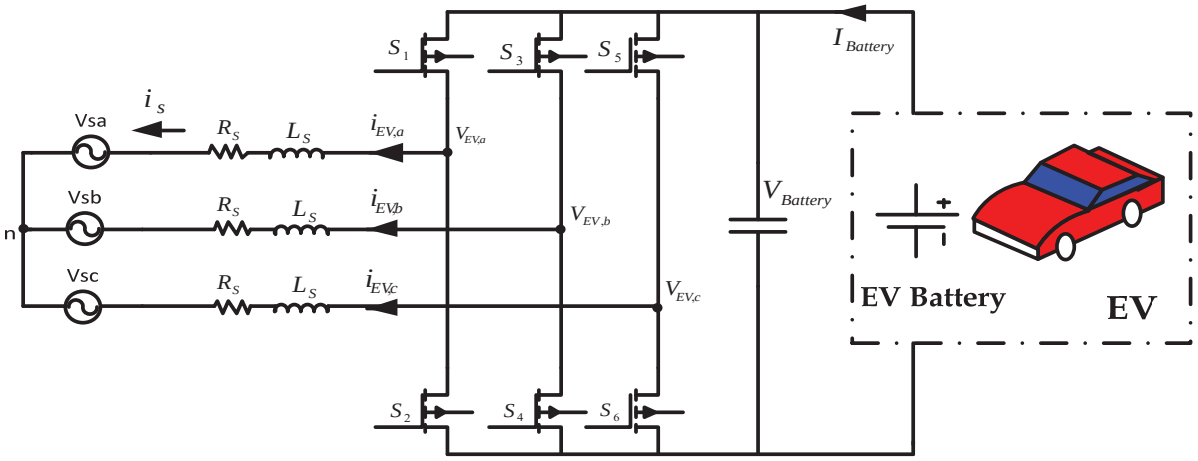

Fig. 1 System structure: the EV is connected to the power grid through an inverter

B. Power Converter Operation

The power converter acts as interface to connect the EV to utility and operates in inverter mode when the EV works in V2G mode. As shown in Fig. 1, the three-phase converter has three legs with two power semiconductor-based switches in each leg. The switches must be appropriately controlled to convert the DC voltage of the battery into an AC voltage with specified frequency (here 50 Hz) of the AC side. However, a pure AC voltage is obtained if appropriate switching signals are implemented. One well known method to control the switches is the space vector modulation (SVM) strategy [27]. In this method, the switching signals Sa, Sb, and Sc determine the switching states of the three-phase converter. These switching signals have logical values; when a switch is *on*, equals one, and when a switch is *off*, equals zero. The switching vector of the converter is defined as;

$$\vec{S} = 2 \setminus 3(S_a + aS_b + a^2 S_c) \quad (3)$$

where $a = e^{j2\pi/3}$. By this definition, the output voltage of the converter of Fig. 1 can be written as;

$$\vec{V}_{EV} = 2/3(V_{EV,a} + aV_{EV,b} + a^2 V_{EV,c}) \quad (4)$$

This voltage is related to the DC voltage of converter, i.e. the EV battery voltage, as;

$$\vec{V}_{EV} = \vec{S} \times V_{Battery} \quad (5)$$

According to the states of the switching signals S_a, S_b, and S_c, eight voltage space vectors are achievable as shown in Table I. From Fig. 1 and using Kirchhoff's Voltage Law (KVL) we have;

$$\vec{V}_{EV} = \vec{V}_s + R\vec{i}_s + L_s \frac{d\vec{i}_s}{dt} + \vec{V}_n \quad (6)$$

where $\vec{V}_s, \vec{i}_s$ are the space vectors of voltage and current of the utility and $\vec{V}_n$ is the space vector of node n that is equal to zero for grounded source point. Thus from (6), we can write;

$$\frac{d\vec{i}_s}{dt} = 1/L_s \left(\vec{V}_{EV} - \vec{V}_s - R\vec{i}_s \right) \quad (7)$$

The discrete form of this equation is used in the next section in the MPC algorithm.

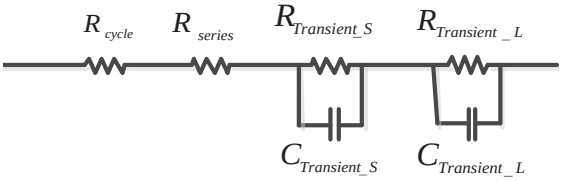

Fig. 2 Equivalent impedance circuit of battery [26]

TABLE I
SPACE PHASOR OF VOLTAGE FOR THE EV INVERTER

Status of switching			Space phasor of voltage
S_a	S_b	S_c	$\vec{V}_{EV}$
0	0	0	$\vec{V}_0 = 0$
0	0	1	$\vec{V}_1 = -V_{Battery}(1/3 + j1/\sqrt{3})$
0	1	0	$\vec{V}_2 = V_{Battery}(-1/3 + j1/\sqrt{3})$
0	1	1	$\vec{V}_3 = -2/3V_{Battery}$
1	0	0	$\vec{V}_4 = 2/3V_{Battery}$
1	0	1	$\vec{V}_5 = V_{Battery}(1/3 - j1/\sqrt{3})$
1	1	0	$\vec{V}_6 = V_{Battery}(1/3 + j1/\sqrt{3})$
1	1	1	$\vec{V}_7 = 0$

III. The MPC Based Control Strategy of EV as a Virtual Active Filter

Fig. 3 shows the overall diagram of the proposed strategy. As shown, the EV is connected in parallel with a non-linear load. The power converter of the EV is controlled based on MPC algorithm that generates the optimal switching signals Sa, Sb, and Sc. The reference currents are obtained from active and reactive power reference calculation in dq frame. To obtain the optimal switching state to be applied for firing the converter switch, a selection criterion must be defined that is the error between references and predicted values. Then, the state that minimizes the errors is selected for the next sampling interval.

A. Current Prediction in MPC

In order to predict the current, it is necessary to transform the dynamic system of the converter for inverter mode of operation represented (7) into discrete time model at sampling time Ts. Thus, a discrete time model is used to predict the future values of currents and voltages in the next sampling interval (n+1), from the measured currents and voltages at the nth sampling instant. Using the system model derivative dy/dt from Euler approximation, as [28];

$$dy/dt = y(n+1) - y(n) \tag{8}$$

The discrete time model of predictive currents and voltages for the next (n+1) sampling instant of the converter during inverter mode can be derived as;

$$\vec{i}_s(n+1) - \vec{i}_s(n) = T_s/L_s\left(\vec{V}_s(n) - \vec{V}_{EV}(n)\right) - R_sT_s/L_s\left(\vec{i}_s(n)\right) \tag{9}$$

So we have;

$$\vec{i}_s(n+1) = \left(1 - R_sT_s/L_s\right)\vec{i}_s(n) + T_s/L_s\left(\vec{V}_s(n) - \vec{V}_{EV}(n)\right) \tag{10}$$

The error function can also be determined as;

$$\vec{e}_d = \left|\vec{i}_d^{\,*} - \vec{i}_d^{\,p}\right| \tag{11}$$

$$\vec{e}_q = \left|\vec{i}_q^{\,*} - \vec{i}_q^{\,p}\right| \tag{12}$$

where $\vec{i}_p^{\,p}$, $\vec{i}_q^{\,p}$ are the dq components of the predicted current.

B. Reference Powers Currents Calculation

Fig. 4 illustrates the process of generating the active and reactive reference powers. The active and reactive power components are calculated as;

$$P = 3/2(v_d i_d + v_q i_q) \tag{13}$$

$$Q = 3/2(-v_d i_q + v_q i_d) \tag{14}$$

As indicated in Fig. 4, based on the equations above, the active and reactive powers that must be compensated are selected. Then, based on these calculated powers, the reference currents in dq frame, i.e. i_d^*, i_q^*, are calculated as;

$$i_d^* = 2/3\left(\frac{V_{sd}}{V_{sd}^2 + V_{sq}^2}\right)P^* + 2/3\left(\frac{V_{sq}}{V_{sd}^2 + V_{sq}^2}\right)Q^* \tag{15}$$

$$i_q^* = 2/3\left(\frac{V_{sq}}{V_{sd}^2 + V_{sq}^2}\right)P^* - 2/3\left(\frac{V_{sd}}{V_{sd}^2 + V_{sq}^2}\right)Q^* \tag{16}$$

These equations indicate that P and Q can be independently controlled and this is a salient feature of the dq frame based control strategies.

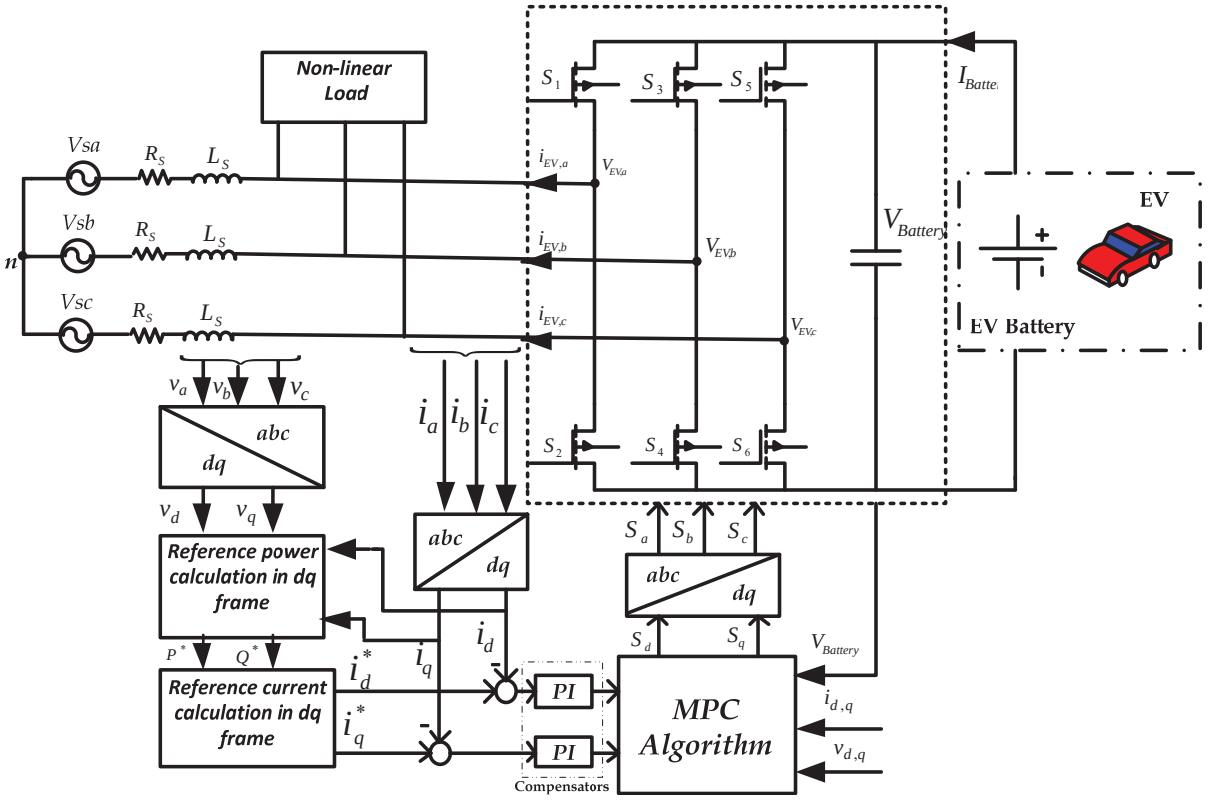

Fig. 3 Proposed MPC based virtual active filter

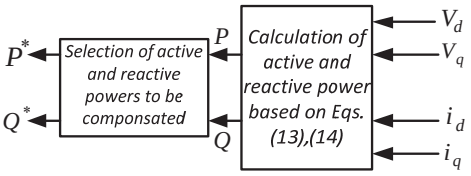

Fig. 4 Active and reactive power reference calculation

IV. Simulation Results

In this section, the virtual active filter is simulated using MATLAB/Simulink [29]. The simulation model is based on Fig. 3 and the parameters of the system are given in Table II, in the Appendix. For purpose of comparison, three case studies have been considered. In these cases, a three phase diode rectifier, with a 10 Ω resistive load, is considered as a nonlinear load. In the first case, there is no any filter used and the load is connected to the utility. In the second case, the method of [24] which was based on p-q theory, is picked up and simulated to improve the power quality when the aforementioned nonlinear load is connected to the power system. Finally, in the third case, the EV is connected to the system and the proposed MPC based strategy is implemented.

Case 1: In this case, the behavior of the nonlinear load and its impact on the power quality is analyzed without harmonic filter. The results are shown in Figs. 5-8. The load is nonlinear and also there are two switching between 0 and 0.01 Seconds. Fig. 5 shows the source current. As illustrated, the phase currents are no sinusoidal and also unbalanced. The neutral current is also shown in Fig. 6. The peak of this current is about 200% more than that of phase *a*. Fig. 7 shows the frequency analysis of the source current. As shown, there are resonances in frequencies of 0 and ±200 Hz and the magnitude in both positive and negative sections of the curve are also high. The Fast Fourier Transform (FFT) analysis of the source current is shown in Fig. 8. It is observed that the magnitude of the third harmonic is 130% respected to the fundamental component. The magnitude of the other harmonics is less than 5%. The THD is also 130.34% which is extremely high.

Case 2: For purpose of comparison, here, the method of [24] is considered. The control scheme of the power converter of EVs is based on p-q theory and the EVs are integrated act as an active filter to improve the power quality. This filter is connected in parallel with the nonlinear load. The simulation results are illustrated in Figs. 9-12. The current source for the phases a, b, and c is indicated in Fig. 9. In comparison with Fig. 5, in which the current of the nonlinear load without any filter is demonstrated, the waveform of the source current is less affected by the load and the distortion is reduced. However, as shown in Fig. 10, the neutral current is notable and its magnitude is high. This is because of the unsymmetrical waveform of the three-

phase current of the source. Fig. 11 shows the frequency analysis of the source current. Again, similar to the case I, the peaks in the frequencies of 0 and ±200 Hz are high. The harmonic spectrum of the source current is also illustrated in Fig. 12. The THD is 8.59% that is higher than the 5% level set by the international standard IEEE 519-2014. One may note that, beside the high amplitude of the third harmonic, the magnitude of other harmonics is notable in the source current. This is mainly because of using the hysteresis band and hysteresis control strategy that was implemented in the p-q theory in [24].

Case 3: The performance of the VAPF is analyzed in this case. The load is the nonlinear load, as it was considered in the previous cases. The VAPF is connected in parallel with the load. The VAPF is controlled using the MPC based strategy of Fig. 3. The simulation results are shown in Figs. 13-17. Fig. 13 shows the source currents. As illustrated, the distortion of these currents is more improved than that of Figs. 5 and 9. The distortion at the initial times, are exist due to the multiple switching. Fig. 14 shows the neutral current that is near to zero for the post switching period. The currents of the VAPF are demonstrated in Fig. 15. The summation of these currents with the load current is such that the harmonics of the load currents are compensated at the source point of view. Fig. 16 indicates the frequency analysis of the source current and the reduction of magnitude is notable. The FFT analysis of the source current is illustrated in Fig. 17 and it is realized that the third harmonic is removed and the THD is reduced to 1.56% which is remarkable and it keeps the IEEE standard limits.

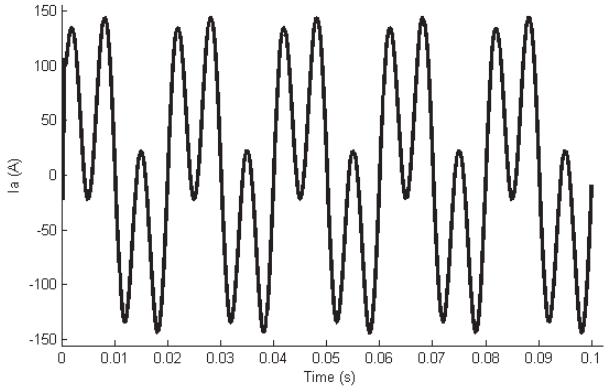

(a) Phase *a* current

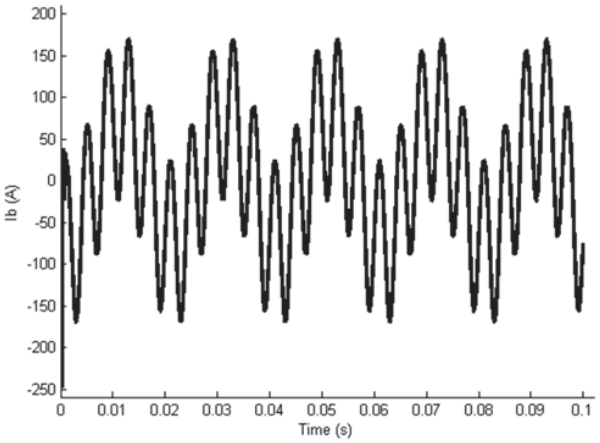

(b) Phase *b* current

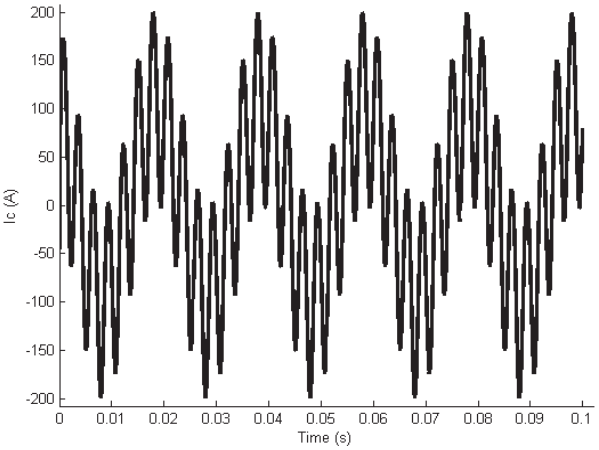

(c) Phase *c* current

Fig. 5 Three phase currents of the source without filter

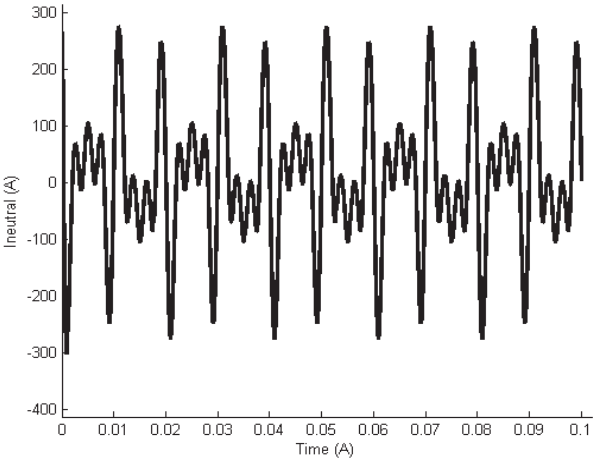

Fig. 6 Neutral current without filter

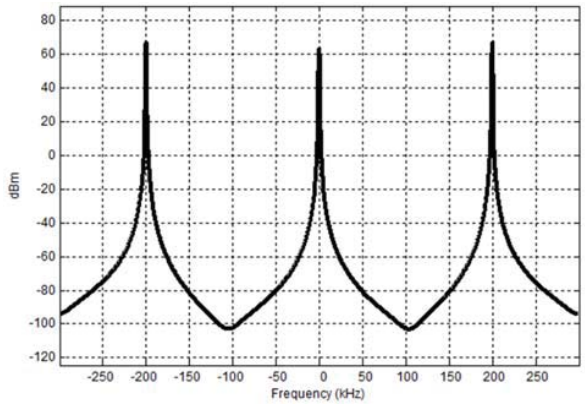

Fig. 7 Frequency spectrum of the source current without filter

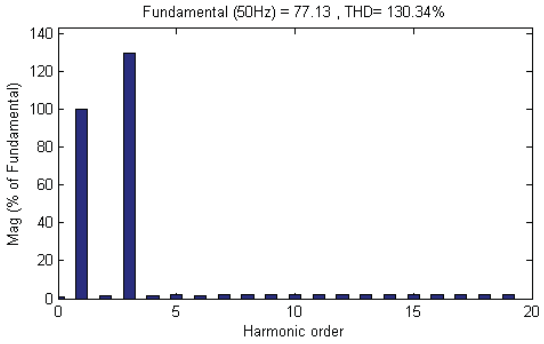

Fig. 8 FFT analysis of the source current without filter

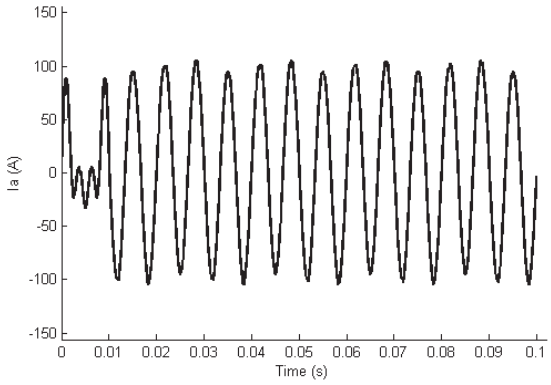

(a) Phase *a* current

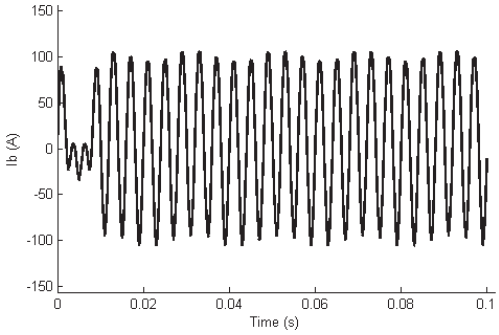

(b) Phase *b* current

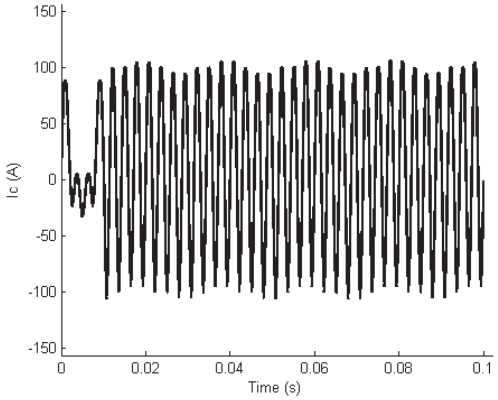

(c) Phase *c* current

Fig. 9 Three phase currents of the source when the method of [24] was implemented

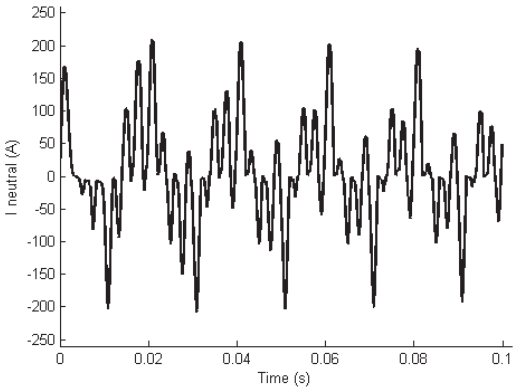

Fig. 10 The neutral current when the method of [24] was implemented

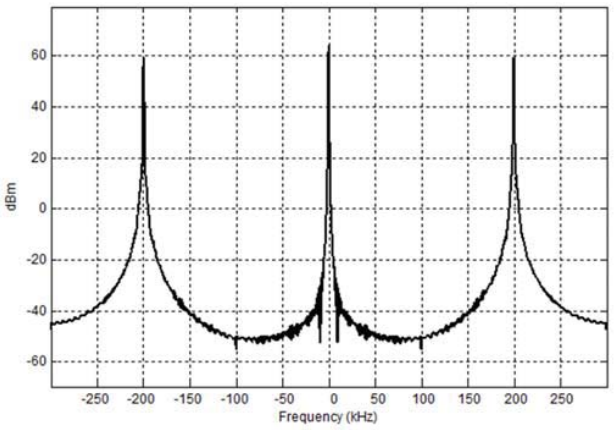

Fig. 11 Frequency spectrum of the source current when the method of [24] was implemented

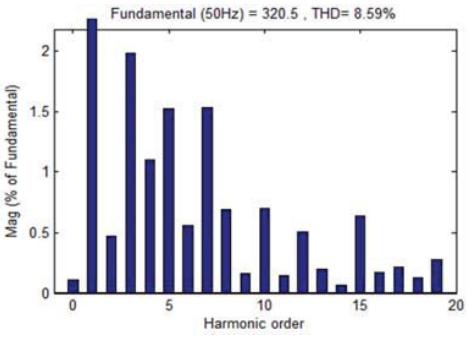

Fig. 12 FFT analysis of the source current when the method of [24] was implemented

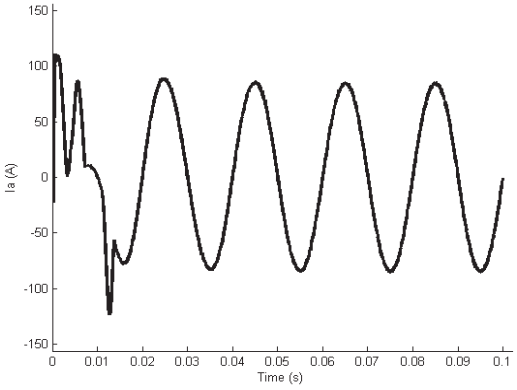

(a) Phase *a* current

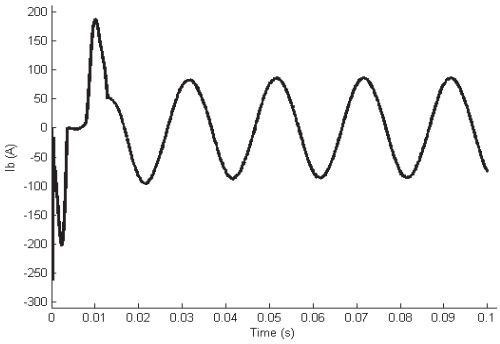

(b) Phase *b* current

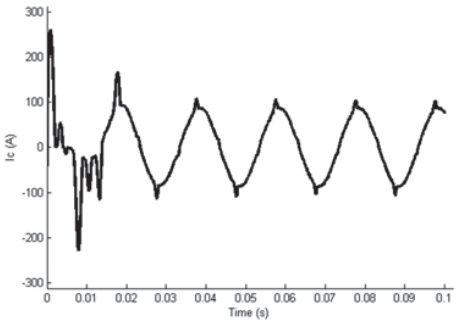

(c) Phase *c* current

Fig. 13 Three phase currents of the source the proposed VAPF

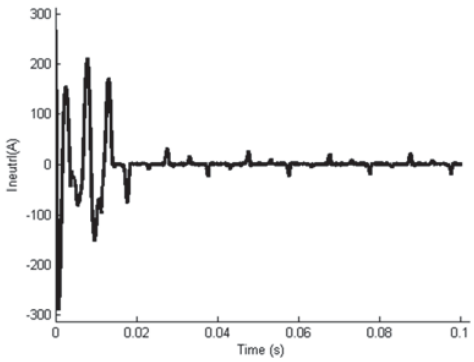

Fig. 14 The neutral current with the proposed VAPF

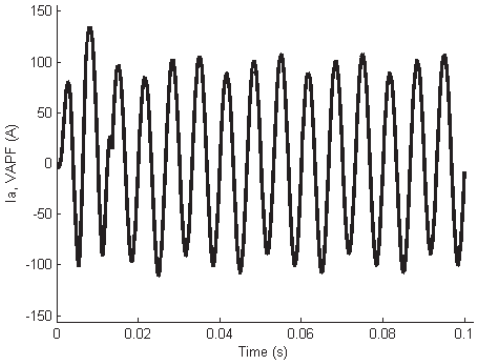

(a) Phase *a* current

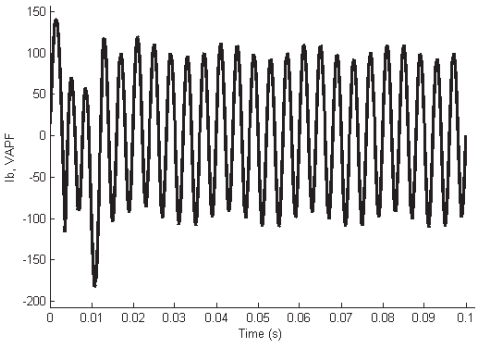

(b) Phase *b* current

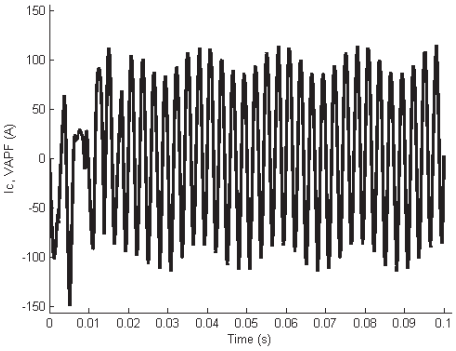

(c) Phase *c* current

Fig. 15 Three phase currents of the proposed VAPF

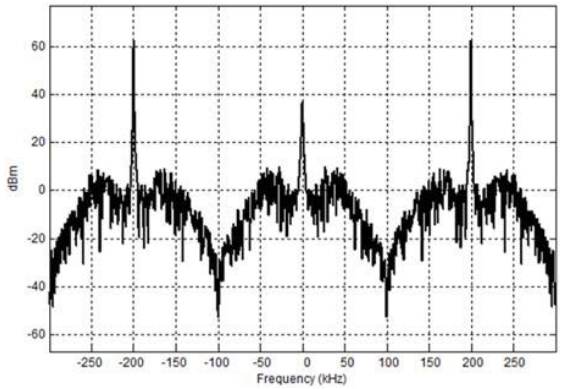

Fig. 16 Frequency spectrum of the source current with the proposed VAPF

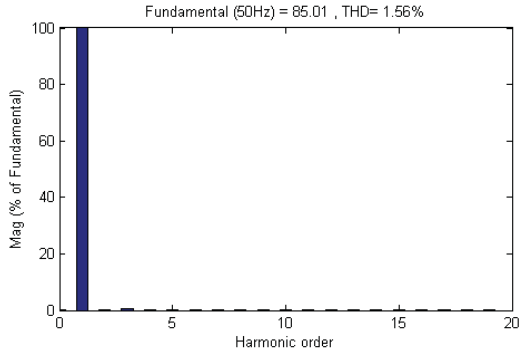

Fig. 17 FFT analysis of the source current with the proposed VAPF

The values of parameters considered in the simulation are given in Table II.

TABLE II
PARAMETERS OF THE SIMULATION MODEL

Parameter	Value
V_s (L-L)	380
f_s	50 Hz
R_s	0.01 Ω
L_s	1 μH
$V_{Battery}$	400 V
K_{PI} (PI controller proportional gain)	0.5
I_{PI} (PI controller integral gain)	1
R_{Load}	10 Ω

V. CONCLUSION

EVs may profitably provide power to the grid at parking lot. This process is called V2G technology. The power converter of the EV can be effectively controlled so that some power quality issues improved. In this respect, the present paper presented a VAPF role for the EV using a MPC based algorithm. The algorithm was effectively able to anticipate the current and determine the optimal switching strategy for the power converter of the EV such that the harmonics are reduced. The results were validated through simulations.

REFERENCES

[1] Singh B, Al-Haddad K, A.Chandra. "*A review of active power filters for power quality improvement*", IEEE Transaction on Industrial Electronics, Vol. 45, No.5, pp. 960–971, 1999.
[2] Ganguly S., "*Impact of unified power-quality conditioner allocation on line loading, losses, and voltage stability of radial distribution systems*", IEEE Transaction on Power Delivery, Vol. 29, No. 4, pp. 1859-1869, 2014.
[3] Khadkikar V., "*Enhancing electrical power quality using UPQC: A comprehensive overview*", IEEE Transaction on Power Electronics, Vol. 27, No. 5, p. 2284–2297, 2012.
[4] Kesler M, Ozdemir E., "*Synchronous-reference-frame-based control method for UPQC under unbalanced and distorted load conditions*", IEEE Transaction on Industrial Electronics, Vol. 58, No. 9, pp. 3967 – 3975, 2011.
[5] Heydari H, Moghadasi AH., "*Optimization scheme in combinatorial UPQC and SFCL using normalized simulated annealing*", IEEE Transaction on Power Delivery, Vol.26, No. 3, pp. 1489 – 1498, 2011.
[6] Khadkikar V, Chandra A. UPQC-S, "*A novel concept of simultaneous voltage sag/swell and load reactive power compensations utilizing series inverter of UPQC*", IEEE Transaction on Power Electronics, Vol. 26, No. 9, pp. 2414–2425, 2011.
[7] Khadkikar V, Chandra A, Barry AO, Nguyen TD., "*Power quality enhancement utilizing single-phase unified power quality conditioner: digital signal processor-based experimental validation*", IET Power Electronics, Vol.4:, No. 3, pp. 323–331, 2011.
[8] Bhattacharya A, Chakraborty C., "*A shunt active power filter with enhanced performance using ANN-based predictive and adaptive controllers*", IEEE Transaction on Industrial Electronics", Vol. 58, No. 2, pp. 421 – 428, 2011.
[9] Senthilkumar A, Ajay-D-Vimal Raj P., "*ANFIS and MRAS-PI controllers based adaptive-UPQC for power quality enhancement application*", Electric Power Systems Research", Vol. 126, No. 1, pp. 1 – 11, 2015.
[10] Singh BN, Singh B, Chandra A, Al-Haddad K., "*Digital implementation of fuzzy control algorithm for shunt active filter*", European Transaction on Electric Power, Vol. 10, No.6, pp. 369-375, 2000.
[11] Pouresmaeil E, et al., "*Instantaneous active and reactive current control technique of shunt active power filter based on the three-level NPC inverter*", European Transaction on Electric Power, Vol. 21, No.7, pp.2007e2022, 2011.
[12] Mikkili S, Panda A K., "*Performance analysis and real-time implementation of shunt active filter Id-Iq control strategy with type-1 and type-2 FLC triangular M.F.*", Int Trans Electr Energy Syst Article, DOI: 10.1002/etep.1698.
[13] W. Kempton, S. Letendre, "*Transportation Research D"* 2, pp.157–175, 1997.
[14] W. Kempton, T. Kubo, "*Energy Policy"* 28, pp.9–18, 2000.
[15] S. Letendre, W. Kempton, "*Public Utilities Fortnightly*" 140, pp.16–26, 2002.
[16] D. Hawkins, *Presentation at the EVAA Electric Transportation Industry Conference*, Sacramento, CA, 13 December, 2001, Presentation slides available at: http://www.acpropulsion.com/reports/Hawkins ETI.pdf.
[17] A. Brooks, *Presentation at the EVAA Electric Transportation Industry Conference*, Sacramento, CA, 13 December, 2001, Presentation slides available at: http://www.acpropulsion.com/reports/A%20Brooks% 20ETI%20conf.pdf.
[18] T. Lipman, J. Edwards, D. Kammen, "*Economic Implications of Net Metering for Stationary and Motor Vehicle Fuel Cell Systems in California*", University of California, Berkeley, 2002, Available at: http://socrates.berkeley.edu/~rael/papers.html#fuelcells.
[19] W. Kempton, J. Tomi´c, J., "*Power Sources*", 144, pp. 280–294, 2005.
[20] Mitra P, Venayagamoorthy G, Corzine K. "*Smart Park as a virtual STATCOM*", IEEE trans on smart grid, Vol. 2, No. 3, pp. 445–455, 2011.
[21] Islam FR, Pota HR., "*PHEVs park as virtual UPFC*", TELKOMNIKA Indones J Electr Eng; Vol. 10, No. 8, pp. 2285–94, 2012.
[22] Guille C, Gross G., "*A conceptual framework for the vehicle to grid V2G implementation*", Energy Policy; Vol. 37, No. 11, pp. 4379–90, 2009.
[23] Islam, FR, Pota HR., "*V2G technology to improve wind power quality and stability*", Australian control conference (AUCC), pp. 452–457, 2011.
[24] F.R. Islam, H.R. Pota, "*Virtual active filters for HVDC networks using V2G technology*", Vol. 54, pp. 399–407, 2014.

[25] Lemoine DM, Kammen DM, Farrell AE., "*An innovation and policy agenda for commercially competitive plug in hybrid electric vehicles*", Environ Res Lett, Vol. 3, No. 1, 014003, 2008.
[26] O. Erdinc, B. Vural and M. Uzunoglu, " *A dynamic lithium-ion battery model considering the effects of temperature and capacity fading*", IEEE, Clean Electrical Power, International Conference on., 2009.
[27] Sanjay Lakshminarayanan, et.al, "*Twelve-Sided Polygonal Voltage Space Vector Based Multilevel Inverter for an Induction Motor Drive With Common-Mode Voltage Elimination*", IEEE Transactions on Industrial Electronics, Vol. 54, No. 5, pp. 2 761 – 2768, 2007.
[28] Bemri H'mida, Soudani Dhaou, "*Discretization of linear continuous systems with input output time delay*", IEEE, 7th International Conference on Modeling, Identification and Control (ICMIC), 2015.
[29] The Mathworks, "*MATLAB/SIMULINK*", R2013b, Version 8.2.0.701.

Mahdi Zolfaghari was born in Aleshtar, Lorestan, Iran, in 1987. Currently, he is a Ph.D. student in electrical engineering at Department of Electrical Engineering, Amirkabir University of Technology (Tehran Polytechnic), Tehran, Iran. He is a member of Iranian Inventors Association (IIA). His research interests include smart grids, renewable energy, power system optimization, robust control and uncertain systems analysis.

Seyed Hossein Hosseinian was born in 1961 in Iran. He received the B.Sc. and M.Sc. degrees from the Electrical Engineering Department of Amirkabir University of Technology (AUT), Tehran, Iran, in 1985 and 1988, respectively, and the Ph.D. degree from the Electrical Engineering Department, University of Newcastle, Newcastle upon Tyne, U.K., in 1995. Presently, he is an Associate Professor in the Electrical Engineering Department at AUT. His special fields of interest include transient in power systems, power quality, restructuring, and deregulation in power systems.

Hossein Askarian Abyaneh (SM'09) was born in Abyaneh, Iran, on March 20, 1953. He received the B.S. and M.S. degrees in Iran in 1976 and 1982, respectively, and the M.S. and Ph.D. degrees in electrical power system engineering from the University of Manchester Institute of Science and Technology, Manchester, U.K., in 1985 and 1988, respectively. He is currently a Professor and the Head of the Department of Electrical Engineering, Amirkabir University of Technology, Tehran, Iran, where he is working in the area of the relay protection and power quality.

M. Abedi received the B.Sc., M.Sc. and Ph.D. degrees from Tehran University, Iran, London University, UK, and Newcastle University, UK, in 1970, 1973, and 1977, respectively. He worked for G.E.C. (U.K) until 1978. Since then he joined EE Dept of Amirkabir University (Tehran, Iran) where he is now professor and head of the Center of Excellence on Power System. Prof. Abedi has published more than 20 books and 140 papers in journals and conferences. He is distinguished professor in Iran and is prize winner for two outstanding books. He is also member of Iranian Academy of Science and member of CIGRE. His main interest is electrical machines and power systems modeling, operation and control.